



# Right heart chambers geometry and function in patients with the atrial and the ventricular phenotypes of functional tricuspid regurgitation

Diana R. Florescu <sup>1,2,3</sup>, Denisa Muraru<sup>2,4</sup>, Cristina Florescu<sup>1</sup>, Valentina Volpato<sup>2,4</sup>, Sergio Caravita<sup>2</sup>, Elisa Perger<sup>2</sup>, Tudor A. Bălșeanu<sup>3</sup>, Gianfranco Parati<sup>2,4</sup>, and Luigi P. Badano <sup>2,4\*</sup>

<sup>1</sup>Department of Cardiology, University of Medicine and Pharmacy of Craiova, Strada Petru Rareș 2, Craiova 200349, Romania; <sup>2</sup>Department of Cardiac, Neural and Metabolic Sciences, Istituto Auxologico Italiano, IRCCS, S. Luca Hospital Piazzale Brescia 20, 20149 Milan, Italy; <sup>3</sup>Department of Physiology, University of Medicine and Pharmacy of Craiova, Strada Petru Rareș 2, Craiova 200349, Romania; and <sup>4</sup>Department of Medicine and Surgery, University of Milano-Bicocca, Piazza dell'Ateneo Nuovo, 1, 20126 Milano MI, Italy

Received 24 June 2021; editorial decision 27 September 2021; accepted 29 September 2021; online publish-ahead-of-print 8 November 2021

See the editorial comment for this article 'Functional tricuspid regurgitation: challenging the old beliefs', by Karima Addetia and Roberto M. Lang, <https://doi.org/10.1093/ehjci/jeab252>.

## Aims

Atrial functional tricuspid regurgitation (A-FTR) is a recently defined phenotype of functional tricuspid regurgitation (FTR) associated with persistent/permanent atrial fibrillation. Differently from the classical ventricular form of FTR (V-FTR), patients with A-FTR might present with severely dilated right atrium and tricuspid annulus (TA), and with preserved right ventricular (RV) size and systolic function. However, the geometry and function of the right ventricle, right atrium, and TA in patients with A-FTR and V-FTR remain to be systematically evaluated. Accordingly, we sought to: (i) study the geometry and function of the right ventricle, right atrium, and TA in A-FTR by two- and three-dimensional transthoracic echocardiography; and (ii) compare them with those found in V-FTR.

## Methods and results

We prospectively analysed 113 (44 men, age  $68 \pm 18$  years) FTR patients (A-FTR = 55 and V-FTR = 58) that were compared to two groups of age- and sex-matched controls to develop the respective Z-scores. Severity of FTR was similar in A-FTR and V-FTR patients. Z-scores of RV size were significantly larger, and those of RV function were significantly lower in V-FTR than in A-FTR ( $P < 0.001$  for all). The right atrium was significantly enlarged in both A-FTR and V-FTR compared to controls ( $P < 0.001$ , Z-scores  $> 2$ ), with similar right atrial (RA) maximum volume (RAVmax) between A-FTR and V-FTR ( $P = 0.2$ ). Whereas, the RA minimum volumes (RAVmin) were significantly larger in A-FTR than in V-FTR ( $P = 0.001$ ).

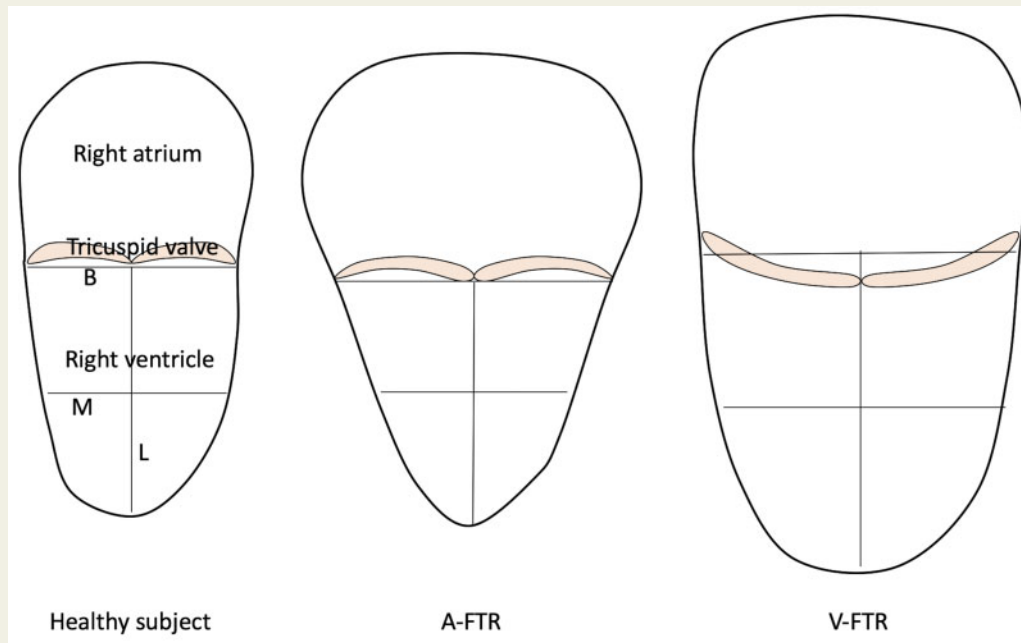
## Conclusion

Despite similar degrees of FTR and RAVmax size, A-FTR patients show larger RAVmin and smaller TA areas than V-FTR patients. Conversely, V-FTR patients show dilated, more elliptic and dysfunctional right ventricle than A-FTR patients.

\* Corresponding author. Tel: +39 375 6119209. E-mail: [luigi.badano@unimib.it](mailto:luigi.badano@unimib.it)

Published on behalf of the European Society of Cardiology. All rights reserved. © The Author(s) 2021. For permissions, please email: [journals.permissions@oup.com](mailto:journals.permissions@oup.com).

## Graphical Abstract



## Keywords

atrial functional tricuspid regurgitation • functional tricuspid regurgitation • tricuspid valve • atrial fibrillation • three-dimensional echocardiography • transthoracic echocardiography

## Introduction

Atrial functional tricuspid regurgitation (A-FTR) is a relatively new phenotype of functional tricuspid regurgitation (FTR).<sup>1</sup> The main mechanism of A-FTR, previously recognized as 'idiopathic FTR', is the progressive dilation and dysfunction of the tricuspid annulus (TA) associated with right atrial (RA) enlargement due to persistent/permanent atrial fibrillation (AF).<sup>2</sup> RA size has been demonstrated to play a crucial role in determining the changes in the tricuspid annular–valvular complex.<sup>3,4</sup> Differently from the classical ventricular form of FTR (V-FTR), patients with A-FTR present with normal/mildly dilated right ventricular (RV) size and preserved RV systolic function.<sup>4,5</sup> However, the geometry and function of the right ventricle, right atrium, and TA in patients with A-FTR and V-FTR remain to be systematically characterized.

Even though the A-FTR and V-FTR overlap in a significant number of patients, the question remains of whether RA and TA dilation might be sufficient for the development of significant FTR in patients with normal RV and systolic pulmonary artery pressure (sPAP). Moreover, identifying the pattern of RV and RA remodelling in the two phenotypes of FTR may be clinically relevant because the assumption that the absence of RV dilation classically indicates milder degrees of FTR<sup>6</sup> might not stand true in A-FTR.

Accordingly, our aims were to (i) study the geometry and function of the right ventricle, right atrium, and TA in A-FTR by two- (2DE) and three-dimensional (3DE) transthoracic echocardiography, and

(ii) to compare them with those found in V-FTR. As a secondary aim, we also sought to evaluate the clinical implications of using 2DE vs. 3DE to assess RV size and function in FTR patients.

## Methods

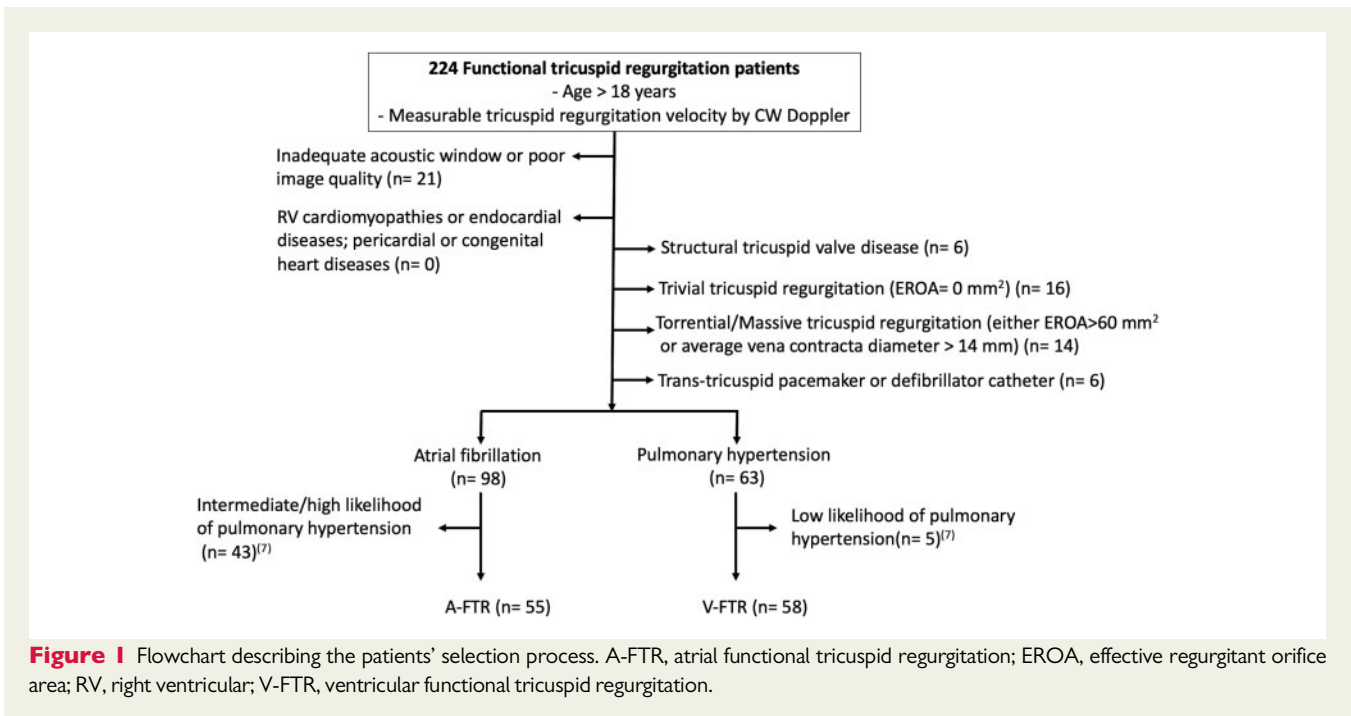
### Study design

We prospectively analysed 2DE and 3DE studies obtained from 224 patients with FTR between July 2020 and May 2021, which were divided into two groups based on the aetiology of FTR (group 1 = persistent/permanent AF and group 2 = pulmonary hypertension (PHTN), PHTN without AF).

The inclusion criteria were: (i) age >18 years; (ii) good quality and complete 2DE and 3DE studies allowing the quantitative assessment of the right ventricle, right atrium, and TA; and (iii) reliable estimation of sPAP by Doppler echocardiography (i.e. well-defined tricuspid regurgitation spectral Doppler tracing and visualization of inferior vena cava throughout the respiratory cycle).<sup>7</sup> The flowchart describing the patients' selection process is shown in *Figure 1*. Subjects included in the control groups were selected among the healthy volunteers enrolled between 2011 and 2014 in the Padua 3D Echo Normal study. Inclusion criteria and clinical characteristics of the healthy subjects, and the results from this project have been published elsewhere.<sup>8–10</sup>

### Echocardiographic acquisition and analysis

We prospectively evaluated patients undergoing clinically indicated transthoracic 2DE and 3DE comprehensive studies using commercially



available Vivid E9, E90, and E95 systems (GE Vingmed, Horten, Norway) equipped with either 4V-D or 4Vc probes.

### The tricuspid valve

The absence of structural tricuspid valve (TV) diseases was checked by obtaining multiple cut-planes from the volume-rendered 3DE dataset of the valve. To grade the severity of FTR, a multi-parametric approach as recommended by current guidelines, using several semi-quantitative and quantitative parameters was used: the average vena contracta (VC) width (measured in apical RV-focused and parasternal long-axis RV inflow views), the proximal isovelocity surface area (PISA) radius of the regurgitant jet at a Nyquist limit of 29 cm/s, the effective regurgitant orifice area (EROA), the regurgitant volume (RVol) using the PISA method, and the regurgitant fraction.<sup>11,12</sup> When indices provided discordant results, the averaged VC width was used for FTR grading.<sup>13</sup> Finally, the size and shape of the TA and leaflets' coaptation place were evaluated using a dedicated software package (4D Auto TVQ, EchoPac v204, GE, Horten, Norway) (Figure 1).<sup>14,15</sup>

### Systolic pulmonary artery pressure

The sPAP was calculated based on the maximum velocity of the continuous-wave Doppler signal of the FTR jet and the RA pressure estimate by inferior vena cava size and inspiratory collapsibility index.<sup>16</sup> The likelihood of PHTN was established based on the peak velocity of the TR jet, and the presence of other echocardiographic signs of PHTN.<sup>7</sup>

### The right ventricle

RV size and function were evaluated using 2DE, 2D speckle-tracking echocardiography, and 3DE. The RV-focused apical views were used to obtain the 2DE RV areas, and diameters. Three RV diameters were measured at end-diastole to assess RV shape. The RV basal diameter was calculated by tracing the largest diameter in the basal third of the right ventricle, parallel to the TA. The RV length was obtained the distance from the centre of the TV annulus to the RV apex. The RV mid-diameter

was measured by tracing a line parallel to the TA and that intersects the RV length at its half.<sup>17</sup> RV free-wall longitudinal strain (RVFWLS) was measured using a dedicated RV strain software (AFI RV, EchoPac v204, GE, Horten, Norway) applied to RV-focused apical views.<sup>18,19</sup> Tricuspid annular plane systolic excursion (TAPSE) was obtained by M-mode from the apical four-chamber view (Figure 2).

RV end-diastolic (EDV) and end-systolic (ESV) volumes, and ejection fraction (EF) were calculated by using 4D Auto RVQ (EchoPac v204, GE, Horten, Norway) on qualitative 3DE datasets (>20 vps<sup>20</sup>). 3DE RV diameters were automatically obtained (Figure 3).

The following ratios between the RV diameters were calculated using both 2DE and 3DE measurements: basal-to-mid, basal-to-length, mid-to-length, and the sphericity index (mid × length/basal diameters).<sup>21</sup>

### The right atrium

RA maximum volume (RAVmax) was calculated by both 2DE (single-plane disk summation method by tracing the endocardial border in RV-focused apical views<sup>17</sup>) and 3DE, and RA minimum volume (RAVmin) by 3DE using a software package developed for the left atrium (4D Auto LAQ, EchoPac v204, GE, Horten, Norway) (Figure 4).

### Reproducibility analysis

Intra- and interobserver reproducibility of 3DE measurements were tested by computing intraclass correlations and coefficients of variation. Intraobserver variability was tested by reanalysing the same beat of 20 qualitative random datasets by the same researcher (D.R.F.) blinded from the initial measurements. The interobserver variability was tested by having the same datasets analysed by a different researcher (V.V.) who was not aware of the results of the other.

### Statistical analysis

Normal distribution of the variables was checked using the Kolmogorov-Smirnov test. Continuous variables were summarized as mean ± standard deviation, and categorical variables were reported as percentages. T-test

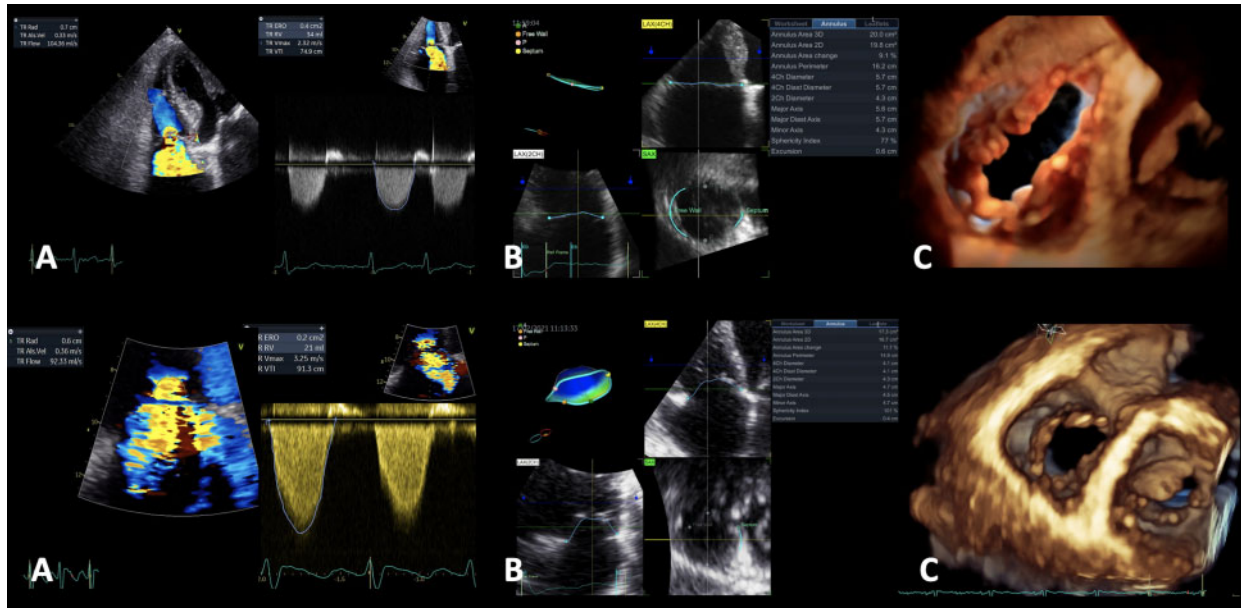


**Figure 2** Functional tricuspid regurgitation assessment and quantification in patients with atriogetic (Top panels) and ventricular (Bottom panels) functional tricuspid regurgitation. (A) Two-dimensional PISA method. (B) Three-dimensional measurement of tricuspid annulus size and shape. (C) Three-dimensional *en face* view of the tricuspid valve anatomy.

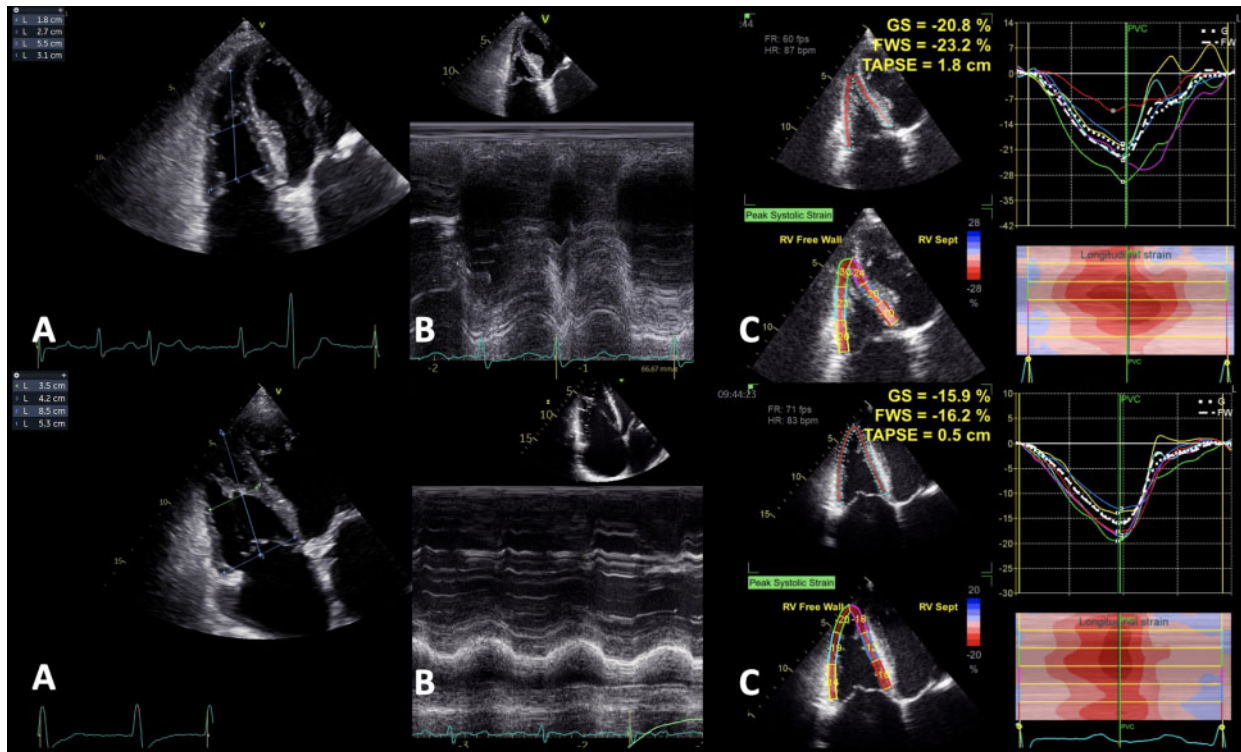


**Figure 3** Right ventricular evaluation by two-dimensional echocardiography. (A) Right ventricular basal, mid and longitudinal diameters' tracing in apical RV-focused view. (B) Measurement of TAPSE using the apical four-chamber view. (C) Right ventricular longitudinal strain calculation using the apical RV-focused views.

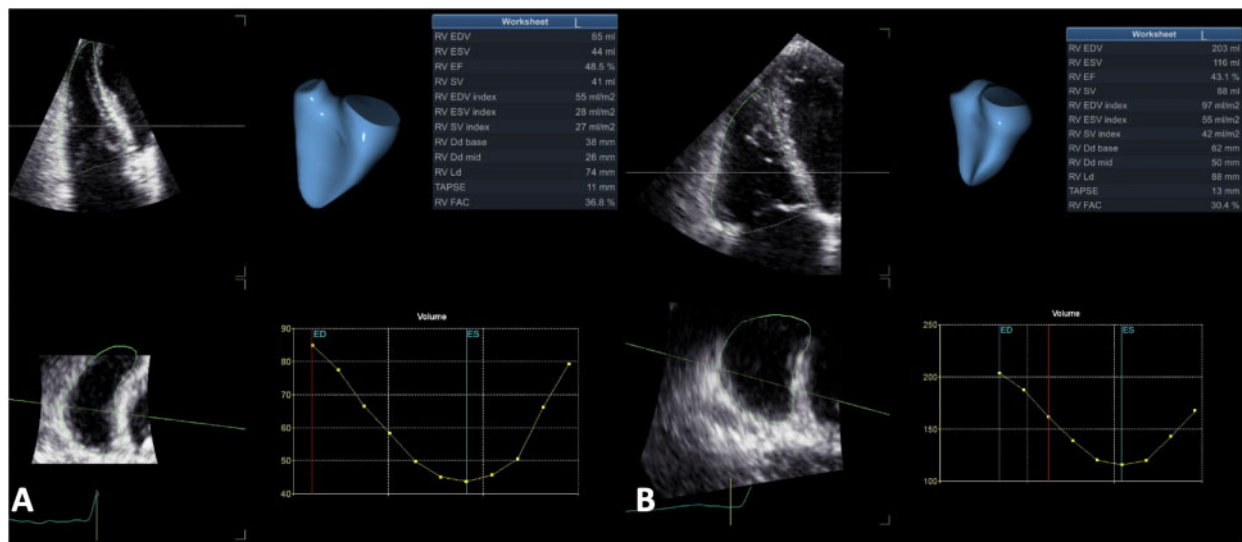


**Figure 4** Three-dimensional right ventricular volumes measurement and ejection fraction calculation. (A) Atriogenic functional tricuspid regurgitation. (B) Ventricular functional tricuspid regurgitation.

for independent variables was used to compare the mean values of the continuous variables, and a  $P$ -value  $<0.05$  was considered statistically significant. Pearson's coefficient of correlation was used for univariate analyses. To test the independent relation between right chambers' volumes and TAAAs, two models of multivariate linear regression were separately performed for A-FTR and V-FTR patients. RAVmax, RAVmin, RVEDV, and RVESV were used as covariates, and TAA at mid-systole (MS) and end-diastole (ED) as dependent variables, respectively. Because patients with A-FTR were significantly older and had a higher prevalence of men than patients with V-FTR, and RV size and function are age-related,<sup>10</sup> and TAA at MS and ED correlate with age and sex in both healthy subjects and FTR patients,<sup>5</sup> Z-scores were computed for intergroup comparison between A-FTR and V-FTR. This was done by including in the Z-scores formula the mean and standard deviation of the analysed parameters of each of the corresponding control groups, reported as values indexed to body surface area. A Z-score  $>2$  was considered significantly abnormal.  $T$ -test was also used to compare the Z-scores between A-FTR patients and A-FTR controls, V-FTR patients and V-FTR controls, and A-FTR and V-FTR groups, respectively. Data analysis was performed using SPSS version 23 statistical software for Mac (SPSS Inc., IBM Corp., Chicago, IL, USA).

## Results

The final study population consisted of 113 FTR patients: 55 patients with lone persistent/permanent AF (A-FTR, age =  $74 \pm 8$  years, 24 men), and 58 patients with PHTN (V-FTR, age =  $61 \pm 18$  years, 19 men) (Figure 1). A-FTR and V-FTR patients were compared to two different control groups (45 A-FTR controls: age =  $71 \pm 9$  years, 20 men; and 46 V-FTR controls: age =  $61 \pm 8$  years, 15 men) matched for age ( $P = 0.068$  and  $0.994$ , respectively) and sex ( $P = 0.920$  and  $P = 0.987$ , respectively). Patients with A-FTR were older, were more frequently men, had larger body size, and higher systolic and diastolic blood pressures than patients with V-FTR (Table 1).

## Tricuspid regurgitation and tricuspid valve geometry in A-FTR and V-FTR patients

The distribution of FTR grading was similar between the A-FTR and the V-FTR patients: mild (27 = 49.1% vs. 23 = 39.7%, respectively), moderate (17 = 30.9% vs. 26 = 44.8%, respectively), and severe (11 = 20% vs. 9 = 15.5%, respectively) ( $P = 0.601$ ). Except for the averaged VC, which was larger in the V-FTR group ( $P = 0.037$ ), all the other quantitative parameters used to grade FTR severity (EROA, PISA radius, RVol, and regurgitant fraction) were similar between A-FTR and V-FTR patients (Table 2). TA systolic area change was similar between A-FTR and V-FTR patients, and significantly reduced compared to controls (Table 2). Moreover, V-FTR patients showed higher coaptation and tenting heights, and a larger tenting volume compared to the A-FTR patients (Table 2).

## The right atrium in A-FTR and V-FTR patients

In both A-FTR and V-FTR patients, 3DE and 2DE RAVmax, and 3DE RAVmin were significantly larger compared to controls (Table 3).

## The right ventricle in A-FTR

A-FTR patients had significantly larger RV basal diameters, shorter RV lengths, and larger RVEDV and RVESV than their controls (Table 3). Moreover, all the parameters of RV function (i.e. RVEF, RVFWLS and TAPSE) were reduced in A-FTR patients compared to controls (Table 3). Moreover, the A-FTR patients had increased basal-to-mid diameter and basal diameter-to-length ratios, while the sphericity index was reduced (Table 3). Conversely, the mid diameter-to-length ratio was similar between A-FTR patients and controls. These changes are consistent with isolated RV basal dilation in A-FTR, resembling a conical shape remodelling pattern (Figure 5).

**Table 1** Baseline characteristics of the study population

	A-FTR	A-FTR controls	P-value	V-FTR	V-FTR controls	P-value
Age (years)	74 ± 8	71 ± 9	0.068	61 ± 18	61 ± 8	0.994
BSA (m <sup>2</sup> )	1.83 ± 0.2	1.73 ± 0.2	0.007	1.71 ± 0.2	1.72 ± 0.2	0.876
Men (%)	24 (45.5)	20 (44.4)	0.920	19 (32.8)	15 (32.6)	0.987
HR (bpm)	76 ± 15	65 ± 10	<0.001	78 ± 14	66 ± 9	<0.001
SBP (mmHg)	135 ± 18	129 ± 12	0.093	119 ± 20	126 ± 16	0.074
DBP (mmHg)	80 ± 14	74 ± 10	0.043	72 ± 11	73 ± 10	0.813
sPAP (mmHg)	28 ± 5	23 ± 5	<0.001	74 ± 14	21 ± 4	<0.001

A-FTR, atrial functional tricuspid regurgitation; bpm, beats per minute; BSA, body surface area; DBP, diastolic blood pressure; HR, heart rate; SBP, systolic blood pressure; sPAP, systolic pulmonary artery pressure; V-FTR, ventricular functional tricuspid regurgitation; y, years.

**Table 2** Parameters used for functional tricuspid regurgitation evaluation

	A-FTR (n = 55)	V-FTR (n = 58)	P-value
Averaged vena contracta width (mm)	4.4 ± 2.1	5.3 ± 1.8	0.037
PISA radius at Nyquist 29 cm/s (mm)	5.5 ± 2.2	6.2 ± 2.2	0.082
Effective regurgitant orifice area (mm <sup>2</sup> )	25 ± 17	22 ± 14	0.195
Regurgitant volume (mL)	20 ± 15	25 ± 16	0.075
Regurgitant fraction (%)	33.5 ± 21	30.3 ± 20	0.424
TA systolic area change (%)	15.5 ± 5.2	14.9 ± 6	0.594
Coaptation height (cm)	0.55 ± 0.3	0.88 ± 0.3	<0.001
Tenting height (cm)	0.62 ± 0.2	0.9 ± 0.3	<0.001
Tenting volume (mL)	2.3 ± 2.4	3.5 ± 2	0.003

2D, two-dimensional; 3D, three-dimensional; A-FTR, atrial functional tricuspid regurgitation; PISA, proximal isovelocity surface area; TA, tricuspid annulus; V-FTR, ventricular functional tricuspid regurgitation.

## The right ventricle in V-FTR

In patients with V-FTR, the RV basal and mid diameters, and the RV length were larger than in controls (Table 3). Both RVEDV and RVESV were larger, and RVEF, RVFWLS, and TAPSE lower in the V-FTR group compared to the controls ( $P < 0.001$  for all, Table 3). Moreover, V-FTR patients showed increased basal-to-mid, basal-to-length, and mid-to-longitudinal diameter ratios, and sphericity index ( $P < 0.001$  for all) compared to controls (with important RV dilation at all levels—basal, mid-ventricular, and longitudinal) (Table 3). This data are consistent with a spherical or elliptical RV remodelling pattern (Figure 5).

As expected, in both A-FTR and V-FTR patients the RV length measured using the 3DE datasets was significantly longer than the RV length obtained from the 2DE views accounting for a certain foreshortening of the right ventricle in 2DE despite the use of the apical RV-focused view (Table 3).

## The right heart in A-FTR vs. V-FTR

Z-scores analysis revealed that A-FTR patients do not have significantly abnormal RV size and function compared to controls (Table 4). Conversely, V-FTR patients have both significantly larger RV size and decreased RV function compared to controls (Table 4). Accordingly, RV Z-scores were significantly higher in V-FTR than in A-FTR ( $P < 0.001$  for all). The RA size was significantly abnormal in both

A-FTR and V-FTR, with similar RAVmax between the two groups. Conversely, RAVmin was significantly larger in A-FTR than in V-FTR (Table 4). TAA at both ED and MS were significantly abnormal and larger in V-FTR than in A-FTR patients ( $P = 0.01$  and  $P < 0.001$ , respectively, Table 4).

## TAA correlations with right heart chambers in A-FTR vs. V-FTR

At bivariate analyses, in A-FTR patients, TAA at both MS and ED correlated with RAVmin ( $r = 0.733$  and  $r = 0.784$ ), RAVmax ( $r = 0.693$  and  $r = 0.759$ ), RVESV ( $r = 0.561$  and  $r = 0.588$ ), and RVEDV ( $r = 0.466$  and  $r = 0.468$ ) ( $P < 0.001$  for all). Similarly, in V-FTR patients, TAA also correlated at both MS and ED with RVEDV ( $r = 0.674$  and  $r = 0.603$ ), RAVmax ( $r = 0.622$  and  $r = 0.677$ ), RAVmin ( $r = 0.627$  and  $r = 0.690$ ), and RVESV ( $r = 0.604$  and  $r = 0.527$ ) ( $P < 0.001$  for all).

However, at multiple linear regression analysis, in A-FTR patients, TAA at MS had a strong, positive correlation with RAVmin (Beta = 0.996,  $P = 0.017$ ), and TAA at ED showed a weaker correlation with RVESV (Beta = 0.526,  $P = 0.036$ ). Conversely, in V-FTR patients, TAA at both MS (Beta = 0.852,  $P = 0.013$ ) and ED (Beta = 0.771,  $P = 0.023$ ) had a strong and positive correlation with RVEDV, whereas TAA at ED correlated with RAVmin (Beta = 0.480,  $P = 0.032$ ).

**Table 3** Comparison of right ventricular and right atrial size and function between patients with the atrial and ventricular phenotype of functional tricuspid regurgitation and their respective controls

	A-FTR	A-FTR controls	P-value	V-FTR	V-FTR controls	P-value
2D RV basal diameter index (mm/m <sup>2</sup> )	24 ± 4	21 ± 3	<0.001	29 ± 5	20 ± 2	<0.001
2D RV mid diameter index (mm/m <sup>2</sup> )	16 ± 4	16 ± 2	0.952	24 ± 6	15 ± 2	<0.001
2D RV length index (mm/m <sup>2</sup> )	37 ± 5	37 ± 4	0.470	45 ± 6	37 ± 4	<0.001
2D basal-to-mid ratio	1.57 ± 0.2	1.37 ± 0.2	<0.001	1.26 ± 0.18	1.4 ± 0.2	<0.001
2D basal-to-length ratio	0.67 ± 0.1	0.57 ± 0.1	<0.001	0.66 ± 0.09	0.56 ± 0.1	<0.001
2D mid-to-length ratio	0.43 ± 0.1	0.42 ± 0.1	0.495	0.54 ± 0.11	0.4 ± 0.1	<0.001
2D sphericity index	43.3 ± 8.5	47.6 ± 7.8	0.011	61.84 ± 12.7	45.9 ± 8.4	<0.001
3D RV basal diameter index (mm/m <sup>2</sup> )	27 ± 4	26 ± 3	0.106	36 ± 6	25 ± 3	<0.001
3D RV mid diameter index (mm/m <sup>2</sup> )	21 ± 4	22 ± 3	0.155	36 ± 7	21 ± 3	<0.001
3D RV length index (mm/m <sup>2</sup> )	41 ± 5	44 ± 4	0.001	54 ± 7	45 ± 4	<0.001
3D basal-to-mid ratio	1.33 ± 0.1	1.21 ± 0.1	<0.001	1.13 ± 0.1	1.23 ± 0.1	<0.001
3D basal-to-length ratio	0.68 ± 0.1	0.6 ± 0.1	<0.001	0.67 ± 0.1	0.57 ± 0.1	<0.001
3D mid-to-length ratio	0.51 ± 0.1	0.5 ± 0.1	0.286	0.6 ± 0.1	0.47 ± 0.1	<0.001
3D sphericity index	56.3 ± 8.4	62.9 ± 9	<0.001	81.9 ± 12.8	62.8 ± 8.8	<0.001
RV end-diastolic volume index (mL/m <sup>2</sup> )	62 ± 16	57 ± 10	0.045	113 ± 41	57 ± 11	<0.001
RV end-systolic volume index (mL/m <sup>2</sup> )	30 ± 10	23 ± 6	<0.001	65 ± 30	23 ± 6	<0.001
RV ejection fraction (%)	51 ± 6	60 ± 5	<0.001	45 ± 9	59 ± 6	<0.001
RV free-wall longitudinal strain (%)	23 ± 5	28 ± 4	<0.001	17 ± 8	28 ± 3	<0.001
TAPSE (mm)	20 ± 4	24 ± 4	<0.001	18 ± 6	24 ± 4	<0.001
3D RA maximum volume index (mL/m <sup>2</sup> )	60 ± 28	28 ± 6	<0.001	54 ± 21	28 ± 6	<0.001
3D RA minimum volume index (mL/m <sup>2</sup> )	48 ± 26	13 ± 4	<0.001	32 ± 19	12 ± 4	<0.001
2D RA maximum volume index (mL/m <sup>2</sup> )	53 ± 24	24 ± 6	<0.001	55 ± 24	23 ± 6	<0.001

2D, two-dimensional; 3D, three-dimensional; A-FTR, atrial functional tricuspid regurgitation; RA, right atrium; RV, right ventricle; TAPSE, tricuspid annular plane systolic excursion; V-FTR, ventricular functional tricuspid regurgitation.

Moreover, by using a cut-off of either 41 mm or 22 mm/m<sup>2</sup> for defining RV dilation based on the 2DE RV basal diameter,<sup>17</sup> 81.8% of the A-FTR patients, 93.1% of the V-FTR patients, and 30.8% of the controls would have been classified as having a dilated RV. In contrast, based on RVEDV index, using sex- and age-specific threshold values,<sup>10</sup> the prevalence of dilated RV changed drastically (A-FTR = 29.1%, V-FTR = 93.1%, and controls = 0%;  $P < 0.001$  compared to the classification based on RV basal diameter). Among patients with severe A-FTR, 73% showed significant RV dilation. However, in the non-severe A-FTR group, 18% of patients also showed dilated RV. Conversely, all patients with V-FTR showed important RV dilation irrespective of the degree of FTR.

### Inter- and intraobserver reproducibility

All 3DE measurements showed excellent intra- and interobserver reproducibility (Table 5).

## Discussion

To the best of our knowledge, this is the first study to use 3DE to provide a systematic comparison of the right heart chambers and TA geometry and function between patients with A-FTR and V-FTR with similar degrees of FTR. Our main findings can be summarized as follows: (i) although A-FTR patients have larger RV basal diameter and volumes and lower RV systolic function compared to their controls,

they were not significantly abnormal (all Z-scores < 2); (ii) V-FTR patients have significantly abnormal RV diameters and volumes (i.e. all Z-scores > 2), and significantly reduced RV systolic function compared to their controls; (iii) the remodelling pattern of the right ventricle in A-FTR patients resembles a conical deformation shape, characterized by increased basal-to-mid and basal-to-longitudinal diameters' ratios, and reduced sphericity index; (iv) the remodelling pattern of the right ventricle in V-FTR patients is consistent with a spherical or elliptical deformation, with an increase in all diameters' ratios and sphericity index; (v) the right atrium is considerably dilated in both A-FTR and V-FTR, with significantly larger RAVmin in A-FTR compared to V-FTR, despite similar RAVmax; and (vi) TAAs, valvular tethering, tenting height, and volume were substantially higher in V-FTR compared to A-FTR.

### Functional tricuspid regurgitation or regurgitations?

The relatively recent understanding that FTR is a powerful and independent predictor of patients' morbidity and mortality,<sup>22–26</sup> and the development of transcatheter procedures to either repair or replace the TV<sup>27</sup> have fuelled the research about the pathophysiology of FTR and the assessment of its haemodynamic and clinical consequences.<sup>28–31</sup> Recently, we have realized that FTR is not a single pathophysiological condition, but there are several phenotypes with different aetiologies, and likely, different outcomes.<sup>1</sup> On one end of

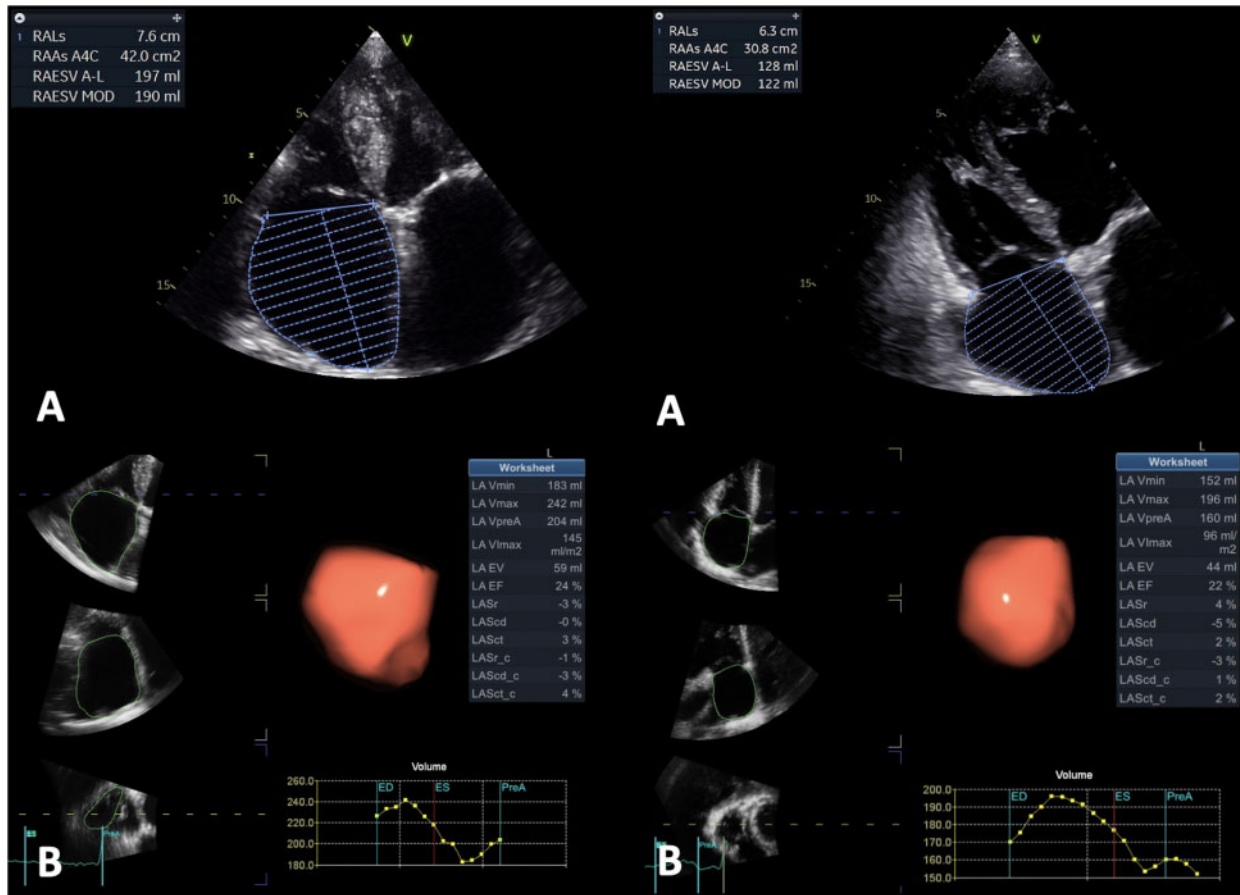


**Figure 5** Right atrial volume quantification measurement in patients with atriogenic (left panels) and ventricular (right panels) functional tricuspid regurgitation. (A) Two-dimensional echocardiography. (B) Three-dimensional echocardiography.

the spectrum, we have patients with A-FTR in whom the main mechanisms leading to regurgitation are supposed to be the dilation and the decrease of the sphincter-like function of the TA, associated to a dilation of the right atrium and an imbalance in the ratio between TA and leaflet areas, typical of patients with persistent/permanent AF.<sup>4,32,33</sup> On the other end of the spectrum, there are the patients with V-FTR in whom the main mechanisms leading to regurgitation are supposed to be the tethering of the leaflets, driven by the dilation/dysfunction of the right ventricle and the consequent displacement and reorientation of the papillary muscles associated to a certain degree of TA dilation, typical of patients with PHTN. However, a systematic comparison of the geometry and function of the right heart structures in A-FTR and in V-FTR patients has never been reported, so far. In our study, we used 3DE to account for the complex shape of the right ventricle, right atrium, and TA.<sup>14,34</sup>

The importance of using 3DE volumetric data to replace linear dimensions to describe the geometry of the right ventricle is underlined by the prevalence of 31% of dilated RV in our healthy volunteers when sized using linear diameters vs. 0% when sized using age- and sex-specific reference ranges for the 3DE RV volumes. Moreover, although we systematically acquired apical RV focus views of the right ventricle, the RV length measured on our

2DE views was systematically shorter than the RV length obtained from the 3DE datasets.

### The right ventricle in A-FTR and V-FTR patients

Topilsky *et al.*<sup>21</sup> studied the RV geometrical changes in patients with idiopathic FTR (id-FTR) and V-FTR (secondary to PHTN). Similar to our findings, id-FTR patients had larger RV basal diameter and shorter RV length. However, in contrast to our results, mid-ventricular diameter was similar between id-FTR and V-FTR. These differences could be explained by the different characteristics of their study population. The prevalence of AF in id-FTR was only 51%, and all three groups (id-FTR, V-FTR, and controls) had similar AF prevalence, questioning the classification of the latter as controls. In our study, we selected only patients with long-persistent/permanent AF to be included in the A-FTR group, and patients with PHTN and sinus rhythm to be included in the V-FTR group. Moreover, we selected two groups of age- and sex-matched healthy volunteers to be compared with A-FTR and V-FTR patients in order to identify more accurately the specific RV changes in A-FTR and V-FTR phenotypes. Finally, due to the crescentic shape of the right ventricle, linear dimensions of RV width depend on the actual position of the tomographic cut plane (i.e.

**Table 4** Comparison of the Z-scores of the echocardiographic parameters describing right ventricular, right atrial, and tricuspid annulus geometry and function between patients with atrial and ventricular phenotype of functional tricuspid regurgitation

Z-scores	A-FTR	V-FTR	P-value
2D RV basal diameter index	1.2 ± 1.5	3.9 ± 2.2	<0.001
2D RV mid diameter index	0.1 ± 1.5	4.0 ± 2.5	<0.001
2D RV length index	-0.2 ± 1.3	2.1 ± 1.5	<0.001
3D RV basal diameter index	0.4 ± 1.3	4.1 ± 2.3	<0.001
3D RV mid diameter index	-0.3 ± 1.3	3.8 ± 2.4	<0.001
3D RV length index	-0.8 ± 1.1	2.3 ± 1.8	<0.001
RV end-diastolic volume index	0.6 ± 1.6	5.3 ± 3.8	<0.001
RV end-systolic volume index	1.3 ± 1.8	7.1 ± 5.2	<0.001
RV ejection fraction	-1.6 ± 1.2	-2.6 ± 1.7	<0.001
3D RA maximum volume index	5.4 ± 4.8	4.4 ± 3.5	0.2
3D RA minimum volume index	9.4 ± 7	5.5 ± 5.1	0.001
2D RA maximum volume index	4.7 ± 4	5.7 ± 4.4	0.214
TA 3D mid-systolic area	2.4 ± 1.3	4.4 ± 3.4	<0.001
TA 3D end-diastolic area	2.4 ± 1.7	3.7 ± 3.3	0.01

2D, two-dimensional; 3D, three-dimensional; RA, right atrium; RV, right ventricle; TA, tricuspid annulus.

degree of probe rotation),<sup>34</sup> by the specific view (four-chamber vs. RV-focused apical view),<sup>35</sup> and by actual RV size.<sup>36</sup>

Using linear dimensions obtained from the 3DE surface rendering of the right ventricle (which have a reproducible inter-patient orientation), we have demonstrated distinct RV remodelling patterns of the right ventricle in the A-FTR and V-FTR patients that explain the morphology of the tricuspid leaflets in these two phenotypes. In patients with A-FTR, there was a prevalent conic deformation of the right ventricle, with enlarged basal dimensions, but preserved length and mid-ventricular transversal diameter. Accordingly, the RV

papillary muscle maintain their position, orientation, and distance from the TV leaflets with minimum tethering of them. The A-FTR is associated to the dilation of the TA, its reduced sphincter function and the imbalance between the TAA and the leaflet area.<sup>32</sup> In patients with V-FTR, there was a spherical or elliptic deformation of the right ventricle that increased in length and in the mid-transversal diameter. This deformation causes displacement and re-alignment of the papillary muscles with a consequent tethering of the TV leaflets. The fact that, despite higher extent of TA dilation in V-FTR, the severity of the regurgitation was similar in patients with A-FTR (minimal valve tenting) and V-FTR (large valve tenting) may be related to ability of the TV leaflets of patients with PHTN to grow in size in response to the systolic stress.<sup>37</sup>

### The right atrium in A-FTR and V-FTR

Similar to our results, Muraru *et al.*<sup>5</sup> reported significant RA and RV dilation in V-FTR, and normal RV volumes in A-FTR. However, differently from our study, in which RAVmax is comparable between two phenotypes, their A-FTR patients had larger RA volumes. The differences might be explained by a higher prevalence of moderate and severe A-FTR in their study. Guta *et al.*<sup>4</sup> found that RAVmin was the main determinant of TAA at both MS and ED. Similarly, in our study, RAVmin had the strongest independent correlation with TAAs in A-FTR. However, in V-FTR, TAAs correlate best with RVEDV, which might explain that despite similar RAVmax and lower RAVmin in V-FTR patients, both TAAs were significantly larger in V-FTR compared to A-FTR.

### RV size as a marker of FTR severity

Current guidelines suggest that an enlarged right ventricle could be used as a supportive sign for severe FTR.<sup>6,38</sup> However, differently from the classical form of V-FTR, we found that A-FTR patients with severe FTR may have normal RV volumes, or on the contrary, patients with less than severe FTR might have dilated RV. Accordingly, in A-FTR the absence of RV dilation should not be considered an indicator of milder degrees of FTR, and the prognosis

**Table 5** Reproducibility of the three-dimensional echocardiographic measurements

	1st measurement	Intra-observer		Inter-observer	
	CV	ICC	CV	ICC	CV
3D RV sphericity index	0.15	0.982	0.14	0.918	0.17
3D RV basal diameter	0.15	0.988	0.14	0.952	0.15
3D RV mid diameter	0.2	0.992	0.19	0.955	0.19
3D RV length	0.09	0.983	0.09	0.805	0.08
RV end-diastolic volume	0.26	0.995	0.26	0.973	0.23
RV end-systolic volume	0.28	0.980	0.29	0.980	0.28
RV ejection fraction	0.11	0.896	0.13	0.846	0.11
RV free-wall longitudinal strain	0.22	0.985	0.21	0.864	0.22
3D RA maximum volume	0.43	0.997	0.45	0.990	0.48
3D RA minimum volume	0.48	0.995	0.51	0.976	0.53
TA 3D mid-systolic area	0.15	0.978	0.15	0.991	0.15
TA 3D end-diastolic area	0.16	0.989	0.16	0.991	0.16

3D, three-dimensional; CV, coefficient of variance; ICC, intra-class correlation coefficient; RA, right atrium; RV, right ventricle; TA, tricuspid annulus.

does not always correlate with the severity of the regurgitation.<sup>39</sup> Accordingly, current TV surgery recommendations in markedly symptomatic patients with severe FTR, or mildly symptomatic in the presence of progressive RV dilation or dysfunction should be weighted taking into account the aetiology of FTR.<sup>40</sup>

## Limitations

Our study enrolled a relatively limited number of patients with A-FTR and V-FTR. This was mainly due to the need of having a well-characterized phenotype for both groups and of avoiding the confounding effect of coexisting pathological conditions. Accordingly, we cannot exclude a selection bias affecting our results that should be confirmed in a larger cohort of patients.

Our results were achieved by using 3DE to quantitate the right heart structures in both patients and controls. We have shown that using 2DE to measure RV and RA size will not necessarily reproduce the same findings. This may reduce the clinical applicability of our results. However, 3DE is the only echocardiographic technique that allows the actual measurement of the complex right heart structures, and our goal was to perform a morphological and pathophysiological study.

## Conclusion

Despite similarly and significantly increased RAVmax, A-FTR patients have larger RAVmin and smaller TAAAs compared to V-FTR. Compared to controls, A-FTR patients have normal RV size and function. Conversely, V-FTR patients present significant RV dilation and dysfunction. These findings provide needed insights on the pathophysiological cascade of the atrial vs. the ventricular phenotype of FTR, and important implications towards specific therapeutic options.

**Conflict of interest:** none declared.

## Data availability

The data underlying this article will be shared on reasonable request to the corresponding author.

## References

- Muraru D, Guta AC, Ochoa-Jimenez RC, Bartos D, Aruta P, Mihaila S *et al*. Functional regurgitation of atrioventricular valves and atrial fibrillation: an elusive pathophysiological link deserving further attention. *J Am Soc Echocardiogr* 2020; **33**:42–53.
- Prihadi EA, Delgado V, Leon MB, Enriquez-Sarano M, Topolsky Y, Bax JJ. Morphologic types of tricuspid regurgitation: characteristics and prognostic implications. *JACC Cardiovasc Imaging* 2019; **12**:491–9.
- Utsunomiya H, Harada Y, Susawa H, Ueda Y, Izumi K, Itakura K *et al*. Tricuspid valve geometry and right heart remodelling: insights into the mechanism of atrial functional tricuspid regurgitation. *Eur Heart J Cardiovasc Imaging* 2020; **21**:1068–78.
- Guta AC, Badano LP, Tomaselli M, Mihalcea D, Bartos D, Parati G *et al*. The pathophysiological link between right atrial remodeling and functional tricuspid regurgitation in patients with atrial fibrillation: a three-dimensional echocardiography study. *J Am Soc Echocardiogr* 2021; **34**:585–94.e1.
- Muraru D, Addetia K, Guta AC, Roberto C, Genovese D, Veronesi F *et al*. Right atrial volume is a major determinant of tricuspid annulus area in functional tricuspid regurgitation: a three-dimensional echocardiographic study. *Eur Heart J Cardiovasc Imaging* 2021; **22**:660–9.
- Lancellotti P, Tribouilloy C, Hagendorff A, Popescu BA, Edvardsen T, Pierard LA *et al*; Scientific Document Committee of the European Association of Cardiovascular Imaging. Recommendations for the echocardiographic assessment of native valvular regurgitation: an executive summary from the European Association of Cardiovascular Imaging. *Eur Heart J Cardiovasc Imaging* 2013; **14**:611–44.
- Galiè N, Humbert M, Vachiery JL, Gibbs S, Lang I, Torbicki A *et al*; ESC Scientific Document Group. 2015 ESC/ERS Guidelines for the diagnosis and treatment of pulmonary hypertension. *Eur Heart J* 2016; **37**:67–119.
- Muraru D, Onciul S, Peluso D, Soriani N, Cucchini U, Aruta P *et al*. Sex- and method-specific reference values for right ventricular strain by 2-dimensional speckle-tracking echocardiography. *Circ Cardiovasc Imaging* 2016; **9**:1–9.
- Peluso D, Badano LP, Muraru D, Dal Bianco L, Cucchini U, Kocabay G *et al*. Right atrial size and function assessed with three-dimensional and speckle-tracking echocardiography in 200 healthy volunteers. *Eur Heart J Cardiovasc Imaging* 2013; **14**:1106–14.
- Maffessanti F, Muraru D, Esposito R, Gripari P, Ermacora D, Santoro C *et al*. Age-, body size-, and sex-specific reference values for right ventricular volumes and ejection fraction by three-dimensional echocardiography: a multicenter echocardiographic study in 507 healthy volunteers. *Circ Cardiovasc Imaging* 2013; **6**:700–10.
- Lancellotti P, Moura L, Pierard LA, Agricola E, Popescu BA, Tribouilloy C *et al*; European Association of Echocardiography. European association of echocardiography recommendations for the assessment of valvular regurgitation. Part 2: mitral and tricuspid regurgitation (native valve disease). *Eur J Echocardiogr* 2010; **11**:307–32.
- Zaidi A, Oxborough D, Augustine DX, Bedair R, Harkness A, Rana B *et al*. Echocardiographic assessment of the tricuspid and pulmonary valves: a practical guideline from the British Society of Echocardiography. *Echo Res Pract* 2020; **7**:G95–122.
- Hahn RT, Thomas JD, Khalique OK, Cavalcante JL, Praz F, Zoghbi WA. Imaging assessment of tricuspid regurgitation severity. *JACC Cardiovasc Imaging* 2019; **12**:469–90.
- Muraru D, Hahn RT, Soliman OI, Faletta FF, Basso C, Badano LP. 3-Dimensional echocardiography in imaging the tricuspid valve. *JACC Cardiovasc Imaging* 2019; **12**:500–15.
- Badano L, Caravita S, Rella V, Guida V, Parati G, Muraru D. The added value of 3-dimensional echocardiography to understand the pathophysiology of functional tricuspid regurgitation. *JACC Cardiovasc Imaging* 2021; **14**:683–6.
- Rudski LG, Lai WW, Afilalo J, Hua L, Handschumacher MD, Chandrasekaran K *et al*. Guidelines for the echocardiographic assessment of the right heart in adults: a report from the American Society of Echocardiography. Endorsed by the European Association of Echocardiography, a registered branch of the European Society of Cardiology, and the Canadian Society of Echocardiography. *J Am Soc Echocardiogr* 2010; **23**:685–713.
- Lang RM, Badano LP, Mor-Avi V, Afilalo J, Armstrong A, Ernande L *et al*. Recommendations for cardiac chamber quantification by echocardiography in adults: an update from the American society of echocardiography and the European association of cardiovascular imaging. *Eur Heart J Cardiovasc Imaging* 2015; **16**:233–71.
- Badano LP, Kollas TJ, Muraru D, Abraham TP, Aurigemma G, Edvardsen T *et al*; Industry representatives; Reviewers: This document was reviewed by members of the 2016–2018 EACVI Scientific Documents Committee. Standardization of left atrial, right ventricular, and right atrial deformation imaging using two-dimensional speckle tracking echocardiography: a consensus document of the EACVI/ASE/Industry Task Force to standardize deformation imaging. *Eur Heart J Cardiovasc Imaging* 2018; **19**:591–600.
- Badano LP, Muraru D, Parati G, Haugaa K, Voigt JU. How to do right ventricular strain. *Eur Heart J Cardiovasc Imaging* 2020; **21**:825–7.
- Muraru D, Spadotto V, Cecchetto A, Romeo G, Aruta P, Ermacora D *et al*. New speckle-tracking algorithm for right ventricular volume analysis from three-dimensional echocardiographic data sets: validation with cardiac magnetic resonance and comparison with the previous analysis tool. *Eur Heart J Cardiovasc Imaging* 2016; **17**:1279–89.
- Topolsky Y, Khanna A, Le Toumeau T, Park S, Michelena H, Suri R *et al*. Clinical context and mechanism of functional tricuspid regurgitation in patients with and without pulmonary hypertension. *Circ Cardiovasc Imaging* 2012; **5**:314–23.
- Benfari G, Antoine C, Miller WL, Thapa P, Topolsky Y, Rossi A *et al*. Excess mortality associated with functional tricuspid regurgitation complicating heart failure with reduced ejection fraction. *Circulation* 2019; **140**:196–206.
- Prihadi EA, Van Der Bijl P, Gursoy E, Abou R, Mara Vollema E, Hahn RT *et al*. Development of significant tricuspid regurgitation over time and prognostic implications: new insights into natural history. *Eur Heart J* 2018; **39**:3574–81.
- Wang N, Fulcher J, Abeysuriya N, McGrady M, Wilcox I, Celermajer D *et al*. Tricuspid regurgitation is associated with increased mortality independent of pulmonary pressures and right heart failure: a systematic review and meta-analysis. *Eur Heart J* 2019; **40**:476–84.

25. Chorin E, Rozenbaum Z, Topilsky Y, Konigstein M, Ziv-Baran T, Richert E et al. Tricuspid regurgitation and long-term clinical outcomes. *Eur Heart J Cardiovasc Imaging* 2020;**21**:157–65.
26. Spinka G, Bartko PE, Heitzinger G, Prausmüller S, Pavo N, Frey MK et al. Natural course of nonsevere secondary tricuspid regurgitation. *J Am Soc Echocardiogr* 2021;**34**:13–9.
27. Voci D, Pozzoli A, Miura M, Gavazzoni M, Gülmez G, Scianna S et al. Developments in transcatheter tricuspid valve therapies. *Expert Rev Cardiovasc Ther* 2019;**17**:841–56.
28. Kebed KY, Addetia K, Henry M, Yamat M, Weinert L, Besser SA et al. Refining severe tricuspid regurgitation definition by echocardiography with a new outcomes-based “massive” grade. *J Am Soc Echocardiogr* 2020;**33**:1087–94.
29. Santoro C, Marco Del Castillo A, González-Gómez A, Monteagudo JM, Hinojar R, Lorente A et al. Mid-term outcome of severe tricuspid regurgitation: are there any differences according to mechanism and severity? *Eur Heart J Cardiovasc Imaging* 2019;**20**:1035–42.
30. Vieitez JM, Monteagudo JM, Mahia P, Perez L, Lopez T, Marco I et al. New insights of tricuspid regurgitation: a large-scale prospective cohort study. *Eur Heart J Cardiovasc Imaging* 2021;**22**:196–202.
31. Muraru D, Previtero M, Ochoa-Jimenez RC, Guta AC, Figliozzi S, Gregori D et al. Prognostic validation of partition values for quantitative parameters to grade functional tricuspid regurgitation severity by conventional echocardiography. *Eur Heart J Cardiovasc Imaging* 2021;**22**:155–65.
32. Muraru D, Caravita S, Guta AC, Mihalcea D, Branzi G, Parati G et al. Functional tricuspid regurgitation and atrial fibrillation: which comes first, the chicken or the egg? *Case (Phila)* 2020;**4**:458–63.
33. Ortiz-Leon XA, Posada-Martinez EL, Trejo-Paredes MC, Ivey-Miranda JB, Pereira J, Crandall I et al. Understanding tricuspid valve remodelling in atrial fibrillation using three-dimensional echocardiography. *Eur Heart J Cardiovasc Imaging* 2020;**21**:747–55.
34. Addetia K, Muraru D, Badano LP, Lang RM. New directions in right ventricular assessment using 3-dimensional echocardiography. *JAMA Cardiol* 2019;**4**:936–44.
35. Genovese D, Mor-Avi V, Palermo C, Muraru D, Volpato V, Kruse E et al. Comparison between four-chamber and right ventricular—focused views for the quantitative evaluation of right ventricular size and function. *J Am Soc Echocardiogr* 2019;**32**:484–94.
36. Surkova E, Muraru D, Aruta P, Romeo G, Bidviene J, Cherata D et al. Current clinical applications of three-dimensional echocardiography: when the technique makes the difference. *Curr Cardiol Rep* 2016;**18**:109.
37. Afilalo J, Grapsa J, Nihoyannopoulos P, Beaudoin J, Gibbs JSR, Channick RN et al. Leaflet area as a determinant of tricuspid regurgitation severity in patients with pulmonary hypertension. *Circ Cardiovasc Imaging* 2015;**8**:1–8.
38. Zoghbi WA, Adams D, Bonow RO, Enriquez-Sarano M, Foster E, Grayburn PA et al. Recommendations for noninvasive evaluation of native valvular regurgitation: a report from the American Society of Echocardiography Developed in Collaboration with the Society for Cardiovascular Magnetic Resonance. *J Am Soc Echocardiogr* 2017;**30**:303–71.
39. Fortuni F, Dietz MF, Prihadi EA, van der Bijl P, De Ferrari GM, Bax JJ et al. Ratio between vena contracta width and tricuspid annular diameter: prognostic value in secondary tricuspid regurgitation. *J Am Soc Echocardiogr* 2021;**34**:944–54.
40. Baumgartner H, Falk V, Bax JJ, de Bonis M, Hamm C, Holm PJ et al.; ESC Scientific Document Group. 2017 ESC/EACTS Guidelines for the management of valvular heart disease. *Eur Heart J* 2017;**38**:2739–86.